Comput. Methods Appl. Mech. Engrg. 199 (2010) 314–323

Contents lists available at ScienceDirect

Comput. Methods Appl. Mech. Engrg.

journal homepage: www.elsevier.com/locate/cma

The importance of the exact satisfaction of the incompressibility constraint in nonlinear elasticity: mixed FEMs versus NURBS-based approximations

F. Auricchio [a,d,e], L. Beirão da Veiga [b,d], C. Lovadina [c,d], A. Reali [a,d,e,*]

[a] Dipartimento di Meccanica Strutturale, Università di Pavia, Italy
[b] Dipartimento di Matematica, Università di Milano, Italy
[c] Dipartimento di Matematica, Università di Pavia, Italy
[d] IMATI-CNR, Pavia, Italy
[e] EUCENTRE, Via Ferrata 1, I-27100, Pavia, Italy

ARTICLE INFO

Article history:
Received 11 January 2008
Received in revised form 21 May 2008
Accepted 11 June 2008
Available online 20 June 2008

Keywords:
Incompressible nonlinear elasticity
Stability
NURBS-based isogeometric analysis
Stream function formulation
Mixed finite elements

ABSTRACT

In the present paper we investigate the capability of finite element methods to correctly reproduce the stability range of finite strain problems in the incompressible regime. To this end, we develop a numerical scheme, obtained combining a stream function formulation with an isogeometric NURBS approach, which is able to sharply estimate the stability limits of the continuous problem. Using such a method, we show a pair of benchmark problems on which various well-known finite element methods largely fail in approximating the correct stability range.

1. Introduction

Despite several finite element schemes perform very well both in terms of accuracy and stability for the case of linear elastic problems, also in the presence of highly constrained situations such as in incompressible cases, it is well known that extensions of such schemes to the case of nonlinear elasticity are not guaranteed to show the same properties in terms of accuracy and/or stability (see, e.g. [18,30]).

In previous works [3,5], we studied the capability of some mixed finite elements (well performing in the small strain regime) to correctly reproduce the stability range of the continuum finite strain problem on a simple model example. The model problem that we selected for our studies consisted of a bidimensional incompressible block, for which a trivial solution could be simply identified. Then, we were able to theoretically find a rough estimate of the stability limit for the continuum problem and to make some comparisons with the results obtained on the discrete problem by means of the mixed finite element schemes under investigation. The conclusions of those works were that all the considered numerical schemes had problems in reproducing the correct continuum stability limit, but a quantitative evaluation of such a failure was missing, since a sharp *theoretical* estimate of the limit for the continuum problem was not available.

In this paper, we study the original model problem proposed in [3] and a new variant obtained considering different boundary conditions. In particular, we show how to construct a reliable estimate for the stability range of the two continuum problems under investigation, which can be used as reference solutions to evaluate in a precise way how a numerical scheme behaves in reproducing the stability properties of the continuum problem. Focusing on the *linearized* problem around a generic solution to the large strain (nonlinear) problem, such an estimate is obtained using an isogeometric "stream function" formulation (see [4]), which allows to exactly enforce the linearized incompressibility constraint. In fact, we show that the exact satisfaction of the linearized incompressibility constraint leads to a numerical approximation of the stability range that converges to the exact one (i.e. the one for the continuum problem). Within this "stream function" context, it is worth noticing that the high regularity of NURBS shape functions [13] is a key ingredient.

A noteworthy result we obtain is that, even with fine meshes, the investigated mixed finite element formulations show traction stability limits which are smaller than the 18% of the expected one in the first example, and smaller than the 35% in the second one. We can therefore conclude that in both cases all the considered mixed finite element schemes completely fail in reproducing

* Corresponding author. Address: EUCENTRE, Via Ferrata 1, I-27100, Pavia, Italy. Tel.: +39 0382 516937; fax: +39 0382 528422.
E-mail address: alessandro.reali@unipv.it (A. Reali).

0045-7825/$ - see front matter © 2008 Elsevier B.V. All rights reserved.
doi:10.1016/j.cma.2008.06.004

the stability range of the continuum problem, despite their small strain counterparts are absolutely reliable.

These conclusions show that, when dealing with highly constrained problems within the finite strain regime, it is not enough using the natural extensions of mixed formulations well performing in small strains, but it is of the highest importance to search for methods able to satisfy the internal constraints in an exact way also in the finite strain context.

A brief outline of the paper is as follows.

In Section 2 we present the (parameter-depending) family of large strain incompressible elasticity problems we are interested in. A mixed variational principle is here used. We then derive the corresponding linearized problems around a generic solution. In addition, for 2D problems, we introduce a *stream function* formulation for the linearized problem (see Section 2.1). In Section 2.2 we present a definition of stability range, which is naturally based on the stability features of the corresponding *linearized* problems. We remark that the stability range can be equivalently defined using both the mixed approach and the stream function formulation.

In Section 3, we state and prove some results about the Galerkin approximation of the stability range. In particular, Proposition 1 concerns the schemes based on the mixed formulation, as the mixed finite element methods presented in Section 5. This result is compatible with the observed phenomenon that mixed finite elements may detect a smaller stability range than the expected one (cf. Remark 2). However, we stress that an efficient approximation of the stability range might be possible for certain particular cases. Proposition 4 concerns the schemes based on the stream function formulation, as the *NURBS approach* presented in Section 5. It is shown that those methods are able to correctly approximate the stability range of the problem at hand (cf. Remark 5).

In Section 4 we provide a description of our two model problems, while Section 5 presents detailed numerical computations, performed with several mixed finite elements and NURBS-based approximation schemes. As already mentioned, numerical tests show a severe failure of the mixed finite elements in approximating the stability range of the corresponding continuous problems.

2. The finite strain incompressible elasticity problem and the stability range

In this paper we adopt the so-called material description to study the finite strain elasticity problem. Accordingly, we suppose that we are given a reference configuration $\Omega \subset \mathscr{R}^d$ for a d-dimensional bounded material body $\mathscr{B}$. Therefore, the deformation of $\mathscr{B}$ can be described by means of the map $\hat{\boldsymbol{\varphi}} : \Omega \to \mathscr{R}^d$ defined by

$$\hat{\boldsymbol{\varphi}}(\mathbf{X}) = \mathbf{X} + \hat{\mathbf{u}}(\mathbf{X}), \tag{1}$$

where $\mathbf{X} = (X_1, \ldots, X_d)$ denotes the coordinates of a material point in the reference configuration and $\hat{\mathbf{u}}(\mathbf{X})$ represents the corresponding displacement vector. Following standard notations (see [7,12,19,21], for instance) we introduce the deformation gradient $\widehat{\mathbf{F}} = \mathbf{F}(\hat{\mathbf{u}})$ and the right Cauchy–Green deformation tensor $\widehat{\mathbf{C}} = \mathbf{C}(\hat{\mathbf{u}})$ by setting

$$\widehat{\mathbf{F}} = \mathbf{I} + \nabla\hat{\mathbf{u}}, \quad \widehat{\mathbf{C}} = \widehat{\mathbf{F}}^{\mathrm{T}}\widehat{\mathbf{F}}, \tag{2}$$

where $\mathbf{I}$ is the second-order identity tensor and ∇ is the gradient operator with respect to the coordinates $\mathbf{X}$.

For a homogeneous neo-Hookean material we define (see for example [7,9]) the potential energy function as

$$\Psi(\hat{\mathbf{u}}) = \frac{1}{2}\mu\left[\mathbf{I} : \widehat{\mathbf{C}} - d\right] - \mu \ln\widehat{J} + \frac{\lambda}{2}(\ln\widehat{J})^2, \tag{3}$$

where λ and μ are positive constants, "$:$" represents the usual inner product for second-order tensors and $\widehat{J} = \det\widehat{\mathbf{F}}$ is the deformation gradient Jacobian.

Introducing the pressure-like variable (or simply pressure) $\hat{p} = \lambda \ln\widehat{J}$, the potential energy (3) can be equivalently written as the following function of $\hat{\mathbf{u}}$ and $\hat{p}$ (still denoted as Ψ with a little abuse of notation)

$$\Psi(\hat{\mathbf{u}}, \hat{p}) = \frac{1}{2}\mu\left[\mathbf{I} : \widehat{\mathbf{C}} - d\right] - \mu \ln\widehat{J} + \hat{p}\ln\widehat{J} - \frac{1}{2\lambda}\hat{p}^2. \tag{4}$$

We wish to study problems whose functionals are of the form

$$\Pi(\hat{\mathbf{u}}, \hat{p}; \gamma) = \int_\Omega \Psi(\hat{\mathbf{u}}, \hat{p}) - \mathscr{F}(\hat{\mathbf{u}}; \gamma), \tag{5}$$

where $\mathscr{F}(\hat{\mathbf{u}}; \gamma)$ represents the work of a family of external loads, smoothly depending on a real parameter γ. In the sequel, we always suppose that $\mathscr{F}(\cdot; \gamma)$ is a *linear* functional for every choice of γ.

According to standard variational principles, equilibrium is derived by searching for critical points of (5) in suitable admissible displacement and pressure spaces $\widehat{U}$ and $\widehat{P}$. The corresponding Euler–Lagrange equations emanating from (5) lead to solve

$$\begin{cases} \text{Find } (\hat{\mathbf{u}}, \hat{p}) \in \widehat{U} \times \widehat{P} \text{ such that} \\ \mu \int_\Omega \widehat{\mathbf{F}} : \nabla\mathbf{v} + \int_\Omega (\hat{p} - \mu)\widehat{\mathbf{F}}^{-\mathrm{T}} : \nabla\mathbf{v} = \mathscr{F}(\mathbf{v}; \gamma) \quad \forall \mathbf{v} \in U \\ \int_\Omega \left(\ln\widehat{J} - \dfrac{\hat{p}}{\lambda}\right) q = 0 \quad \forall q \in P, \end{cases} \tag{6}$$

where U and P are the admissible variation spaces for the displacements and the pressures, respectively. We note that a solution $(\hat{\mathbf{u}}, \hat{p}) \in \widehat{U} \times \widehat{P}$ may obviously depend on the parameter γ, though not explicitly written, for notational simplicity. We also note that in (6) we used that the linearization of the deformation gradient Jacobian is

$$DJ(\hat{\mathbf{u}})[\mathbf{v}] = J(\hat{\mathbf{u}})\mathbf{F}(\hat{\mathbf{u}})^{-\mathrm{T}} : \nabla\mathbf{v} = \widehat{J}\widehat{\mathbf{F}}^{-\mathrm{T}} : \nabla\mathbf{v} \quad \forall \mathbf{v} \in U. \tag{7}$$

We now focus on the case of an *incompressible* material, which corresponds to take the limit $\lambda \to +\infty$ in (6). Hence, our problem becomes:

$$\begin{cases} \text{Problem } (\mathscr{P}_\gamma) : \text{Find } (\hat{\mathbf{u}}, \hat{p}) \in \widehat{U} \times \widehat{P} \text{ such that} \\ \mu \int_\Omega \widehat{\mathbf{F}} : \nabla\mathbf{v} + \int_\Omega (\hat{p} - \mu)\widehat{\mathbf{F}}^{-\mathrm{T}} : \nabla\mathbf{v} = \mathscr{F}(\mathbf{v}; \gamma) \quad \forall \mathbf{v} \in U, \\ \int_\Omega q \ln\widehat{J} = 0 \quad \forall q \in P. \end{cases} \tag{8}$$

We then derive the linearization of problem (8) around a solution $(\hat{\mathbf{u}}, \hat{p})$, corresponding to an increment $\delta\gamma$ of γ. Observing that

$$D\widehat{\mathbf{F}}^{-\mathrm{T}}(\hat{\mathbf{u}})[\mathbf{u}] = -\widehat{\mathbf{F}}^{-\mathrm{T}}(\nabla\mathbf{u})^{\mathrm{T}}\widehat{\mathbf{F}}^{-\mathrm{T}} \quad \forall \mathbf{u} \in U, \tag{9}$$

we easily get the problem for the increment $(\mathbf{u}, p)$

$$\begin{cases} \text{Problem } (\mathscr{LP}_\gamma) : \text{Find } (\mathbf{u}, p) \in U \times P \text{ such that} \\ \mu \int_\Omega \nabla\mathbf{u} : \nabla\mathbf{v} + \int_\Omega (\mu - \hat{p})(\widehat{\mathbf{F}}^{-1}\nabla\mathbf{u})^{\mathrm{T}} : \widehat{\mathbf{F}}^{-1}\nabla\mathbf{v} \\ \quad + \int_\Omega p\widehat{\mathbf{F}}^{-\mathrm{T}} : \nabla\mathbf{v} = \dfrac{\partial}{\partial\gamma}\mathscr{F}(\mathbf{v}; \gamma)\delta\gamma \quad \forall \mathbf{v} \in U, \\ \int_\Omega q\widehat{\mathbf{F}}^{-\mathrm{T}} : \nabla\mathbf{u} = 0 \quad \forall q \in P, \end{cases} \tag{10}$$

where the functional $\dfrac{\partial}{\partial\gamma}\mathscr{F}(\cdot; \gamma) : U \to \mathscr{R}$ is defined by

$$\frac{\partial}{\partial\gamma}\mathscr{F}(\mathbf{v}; \gamma) := \lim_{\Delta\gamma \to 0} \frac{\mathscr{F}(\mathbf{v}; \gamma + \Delta\gamma) - \mathscr{F}(\mathbf{v}; \gamma)}{\Delta\gamma} \quad \forall \mathbf{v} \in U. \tag{11}$$

Setting

$$\begin{cases} a_\gamma(\mathbf{u}, \mathbf{v}) := \mu \int_\Omega \nabla\mathbf{u} : \nabla\mathbf{v} \\ \qquad\qquad + \int_\Omega (\mu - \hat{p})(\widehat{\mathbf{F}}^{-1}\nabla\mathbf{u})^{\mathrm{T}} : \widehat{\mathbf{F}}^{-1}\nabla\mathbf{v} \quad \forall \mathbf{u}, \mathbf{v} \in U, \\ b_\gamma(\mathbf{v}, q) := \int_\Omega q\widehat{\mathbf{F}}^{-\mathrm{T}} : \nabla\mathbf{v} \quad \forall \mathbf{v} \in U \ \forall q \in P. \end{cases} \tag{12}$$

Problem (10) can be written as

$$\begin{cases} \text{Problem } (\mathscr{LP}_\gamma) : \text{Find } (\mathbf{u}, p) \in U \times P \text{ such that} \\ a_\gamma(\mathbf{u}, \mathbf{v}) + b_\gamma(\mathbf{v}, p) = \dfrac{\partial}{\partial\gamma}\mathscr{F}(\mathbf{v}; \gamma)\delta\gamma \quad \forall \mathbf{v} \in U, \\ b_\gamma(\mathbf{u}, q) = 0 \quad \forall q \in P. \end{cases} \tag{13}$$

We remark that the forms $a_\gamma(\cdot,\cdot)$ and $b_\gamma(\cdot,\cdot)$ are dependent on γ, since $\widehat{\mathbf{F}}$ and $\hat{p}$ are so. We also note that problem (13) is a typical (parameter-dependent) saddle-point problem in variational form, where the second equation represents a kinematical constraint for the displacement increment $\mathbf{u}$.

2.1. A "stream function" formulation for Problem $(\mathscr{LP}_\gamma)$

We now present a reformulation of Problem $(\mathscr{LP}_\gamma)$ for which the displacement increment $\mathbf{u}$ automatically satisfies the constraint given by the second equation of (13). We here suppose that Ω is a simply connected domain of $\mathscr{R}^2$. For some hints on possible extensions to three-dimensional and multiply connected cases, see [4]. We first note that the Piola identity $\mathbf{div}(\widehat{J}\widehat{\mathbf{F}}^{-\mathrm{T}}) = \mathbf{0}$ and $\widehat{J} = 1$ give $\mathbf{div}(\widehat{\mathbf{F}}^{-\mathrm{T}}) = \mathbf{0}$. Hence, from the definition of $b_\gamma(\cdot,\cdot)$ in (12) it follows:

$$\operatorname{div}(\widehat{\mathbf{F}}^{-1}\mathbf{v}) = \mathbf{div}(\widehat{\mathbf{F}}^{-\mathrm{T}})\cdot\mathbf{v} + \widehat{\mathbf{F}}^{-\mathrm{T}} : \nabla\mathbf{v} = 0 \quad \forall \mathbf{v}\in K_\gamma, \tag{14}$$

where

$$K_\gamma := \{\mathbf{v}\in U : b_\gamma(\mathbf{v},q) = 0\ \forall q\in P\}. \tag{15}$$

Therefore, given $\mathbf{v}\in K_\gamma$, there exists a "stream function" ψ, defined up to an additive constant, such that

$$\widehat{\mathbf{F}}^{-1}\mathbf{v} = \mathbf{curl}\,\psi \quad \text{i.e. } \mathbf{v} = \widehat{\mathbf{F}}\,\mathbf{curl}\,\psi. \tag{16}$$

We set the *stream function space* as

$$\Phi_\gamma = \{\psi : \widehat{\mathbf{F}}\,\mathbf{curl}\,\psi \in U\}/\mathscr{R}, \tag{17}$$

where the index highlights the dependence of the space definition on the parameter γ (through $\widehat{\mathbf{F}}$).

Introducing the notation

$$\mathbf{curl}_{\widehat{\mathbf{F}}}\psi := \widehat{\mathbf{F}}\,\mathbf{curl}\,\psi, \tag{18}$$

Problem $(\mathscr{LP}_\gamma)$ (see (10)) can thus be written as

$$\begin{cases} \text{Problem } (\mathscr{LP}^*_\gamma) : \text{Find } \varphi\in\Phi_\gamma \text{ such that} \\ a^*_\gamma(\varphi,\psi) = \dfrac{\partial}{\partial\gamma}\mathscr{F}(\mathbf{curl}_{\widehat{\mathbf{F}}}\psi;\gamma)\delta\gamma \quad \forall\psi\in\Phi_\gamma, \end{cases} \tag{19}$$

where

$$\begin{aligned} a^*_\gamma(\varphi,\psi) := \mu\int_\Omega \nabla(\mathbf{curl}_{\widehat{\mathbf{F}}}\varphi) : \nabla(\mathbf{curl}_{\widehat{\mathbf{F}}}\psi) \\ + \int_\Omega (\mu-\hat{p})(\widehat{\mathbf{F}}^{-1}\nabla(\mathbf{curl}_{\widehat{\mathbf{F}}}\varphi))^{\mathrm{T}} : \widehat{\mathbf{F}}^{-1}\nabla(\mathbf{curl}_{\widehat{\mathbf{F}}}\psi). \end{aligned} \tag{20}$$

We remark that *Problem* $(\mathscr{LP}^*_\gamma)$ above corresponds to a *fourth order PDE problem*. We also remark that, once $\varphi\in\Phi_\gamma$ has been found by solving (19), the displacement increment $\mathbf{u}$ can be obtained by computing (cf. (18))

$$\mathbf{u} = \mathbf{curl}_{\widehat{\mathbf{F}}}\varphi. \tag{21}$$

2.2. The stability range

We now make the assumption

$$\mathscr{F}(\mathbf{v};0) = 0 \quad \forall\mathbf{v}\in U, \tag{22}$$

which means to consider a loading–free problem at $\gamma = 0$. Therefore, Problem $(\mathscr{P}_0)$ (see (8)) admits the trivial solution $(\hat{\mathbf{u}},\hat{p}) = (\mathbf{0},0)$. Furthermore, its linearization becomes (cf. (10)):

$$\begin{cases} \text{Problem } (\mathscr{LP}_0) : \text{Find } (\mathbf{u},p)\in U\times P \text{ such that} \\ 2\mu\int_\Omega \boldsymbol{\varepsilon}(\mathbf{u}) : \boldsymbol{\varepsilon}(\mathbf{v}) + \int_\Omega p\operatorname{div}\mathbf{v} = \dfrac{\partial}{\partial\gamma}\mathscr{F}(\mathbf{v};0)\delta\gamma \quad \forall\mathbf{v}\in U, \\ \int_\Omega q\operatorname{div}\mathbf{u} = 0 \quad \forall q\in P, \end{cases} \tag{23}$$

where $\boldsymbol{\varepsilon}(\cdot)$ denotes the symmetric gradient operator. It is well known (see [8], for instance) that Problem (23) corresponds to a well-posed *coercive* constrained problem, the constraint being the divergence-free condition. As a consequence, the trivial solution $(\mathbf{0},0)$ is an *isolated stable* solution to Problem $(\mathscr{P}_0)$. More precisely, the point $(\hat{\mathbf{u}},\hat{p};\gamma) = (\mathbf{0},0;0)$ fits the following definition.

Definition 1. Let $\gamma\in\mathscr{R}$, and let $(\hat{\mathbf{u}},\hat{p})\in U\times P$ be a solution to Problem $(\mathscr{P}_\gamma)$ (see (8)). We say that $(\hat{\mathbf{u}},\hat{p};\gamma)$ is a *linearization stable point* for Problem $(\mathscr{P}_\gamma)$ if the corresponding linearization (13) satisfies:

- *the inf-sup condition*, i.e. it holds

$$\beta_\gamma := \inf_{q\in P}\sup_{\mathbf{v}\in U}\frac{b_\gamma(\mathbf{v},q)}{\|\mathbf{v}\|_U\|q\|_P} > 0; \tag{24}$$

- *the coercivity on the kernel condition*, i.e. it holds

$$\alpha_\gamma := \inf_{\mathbf{v}\in K_\gamma}\frac{a_\gamma(\mathbf{v},\mathbf{v})}{\|\mathbf{v}\|^2_U} > 0. \qquad \square \tag{25}$$

We are now ready to introduce our definition of *stability range*.

Definition 2. We define the *stability range* of Problem $(\mathscr{P}_\gamma)$ as the interval $S(\mathscr{P}_\gamma) = (\gamma_m,\gamma_M)\subseteq\mathscr{R}$, where

$$\begin{cases} \gamma_m = \inf\{\gamma\in\mathscr{R} : \exists \text{ a continuous path of linearization} \\ \qquad \text{stable points joining } (\mathbf{0},0;0) \text{ and } (\hat{\mathbf{u}},\hat{p};\gamma)\}, \\ \gamma_M = \sup\{\gamma\in\mathscr{R} : \exists \text{ a continuous path of linearization} \\ \qquad \text{stable points joining} (\mathbf{0},0;0) \text{ and } (\hat{\mathbf{u}},\hat{p};\gamma)\}. \qquad \square \end{cases} \tag{26}$$

For 2D problems, we notice that using the *stream function* formulation (19), (20), Definition 1 can be rephrased into the following single

- *coercivity condition*: it holds

$$\alpha_\gamma := \inf_{\psi\in\Phi_\gamma}\frac{a^*_\gamma(\psi,\psi)}{\|\psi\|^2_{\Phi_\gamma}} > 0, \tag{27}$$

where

$$\|\psi\|_{\Phi_\gamma} := \|\mathbf{v}\|_U \quad \text{if } \mathbf{v} = \widehat{\mathbf{F}}\,\mathbf{curl}\,\psi \quad (\text{cf. } (16)). \tag{28}$$

Accordingly, the *stability range* of Problem $(\mathscr{P}_\gamma)$ introduced by Definition 2 can be equivalently given in terms of the *stream function* formulation (19) and (20).

A typical stability range is schematically depicted in Fig. 1. We remark that outside the stability range (γ_m,γ_M) we expect multiple solutions of the nonlinear problem (8). Therefore, $\gamma\to\alpha_\gamma$ is a multi-valued function outside (γ_m,γ_M), in general. However, in Fig. 1 a single branch has been displayed, for simplicity.

3. Galerkin approximation of the stability range

In this Section we prove a few results about the numerical approximation of the stability range, as defined by Definitions 1 and 2 (cf. also (27), (28)) when we discretize the continuous problem through a Galerkin approximation. In what follows we will exclusively focus on the stability properties of the discretization of the *linearized Problem* $(\mathscr{LP}_\gamma)$ (see (13)). Therefore, we will always suppose that the analytical solution $(\hat{\mathbf{u}},\hat{p})$ of the non-linear Problem $(\mathscr{P}_\gamma)$, corresponding to γ (see (8)), is *exactly available*. Of course, this assumption is unrealistic in most practical situations, because only an approximation $(\hat{\mathbf{u}}_h,\hat{p}_h)$ of $(\hat{\mathbf{u}},\hat{p})$ is generally at hand. However, it allows a simpler, though meaningful, study on possible discretization troubles.

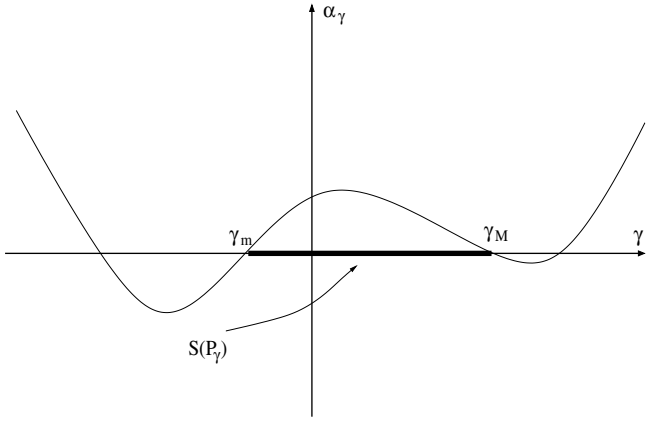

Fig. 1. Stability range.

3.1. Approximation by means of the mixed formulation

We now consider a Galerkin approximation of the linearized problem (13). We thus select a family of finite dimensional subspaces $U_h \subset U$ and $P_h \subset P$ ($h > 0$), with the basic approximation property:

$$\bigcup_{h>0} U_h \text{ is dense in } U, \quad \bigcup_{h>0} P_h \text{ is dense in } P. \tag{29}$$

We then consider the following discrete problem:

$$\begin{cases} \text{Problem } (\mathscr{L}\mathscr{P}_{\gamma,h}) : \text{Find } (\mathbf{u}_h, p_h) \in U_h \times P_h \text{ such that} \\ a_\gamma(\mathbf{u}_h, \mathbf{v}_h) + b_\gamma(\mathbf{v}_h, p_h) = \dfrac{\partial}{\partial\gamma}\mathscr{F}(\mathbf{v}_h;\gamma)\delta\gamma \quad \forall \mathbf{v} \in U_h, \\ b_\gamma(\mathbf{u}_h, q_h) = 0 \quad \forall q_h \in P_h. \end{cases} \tag{30}$$

Within this framework, we can now introduce the discrete counterparts of Definitions 1 and 2.

Definition 3. Let $\gamma \in \mathscr{R}$, and let $(\hat{\mathbf{u}}, \hat{p}) \in U \times P$ be a solution to Problem $(\mathscr{P}_\gamma)$ (see (8)). For a given $h > 0$, we say that $(\hat{\mathbf{u}}, \hat{p}; \gamma)$ is a *discrete linearization stable point* for Problem $(\mathscr{P}_\gamma)$ if the corresponding discrete linearization (30) satisfies:

- *the discrete inf-sup condition*, i.e. it holds

$$\inf_{q_h \in P_h} \sup_{\mathbf{v}_h \in U_h} \frac{b_\gamma(\mathbf{v}_h, q_h)}{\|\mathbf{v}_h\|_U \|q_h\|_P} > 0; \tag{31}$$

- *the discrete coercivity on the kernel condition*, i.e. it holds

$$\inf_{\mathbf{v}_h \in K_{\gamma,h}} \frac{a_\gamma(\mathbf{v}_h, \mathbf{v}_h)}{\|\mathbf{v}_h\|_U^2} > 0, \tag{32}$$

where the discrete kernel $K_{\gamma,h}$ is defined by (cf. (15))

$$K_{\gamma,h} := \{\mathbf{v}_h \in U_h : b_\gamma(\mathbf{v}_h, q_h) = 0 \ \forall q_h \in P_h\}. \tag{33}$$

Definition 4. For a given $h > 0$, we define the *discrete stability range* of Problem $(\mathscr{P}_\gamma)$ as the interval $S_h(\mathscr{P}_\gamma) = (\gamma_{m,h}, \gamma_{M,h}) \subseteq \mathscr{R}$, where

$$\begin{cases} \gamma_{m,h} = \inf\{\gamma \in \mathscr{R} : \exists \text{ a continuous path of discrete linearization} \\ \qquad \text{stable points joining } (\mathbf{0}, 0; 0) \text{ and } (\hat{\mathbf{u}}, \hat{p}; \gamma)\}, \\ \gamma_{M,h} = \sup\{\gamma \in \mathscr{R} : \exists \text{ a continuous path of discrete linearization} \\ \qquad \text{stable points joining } (\mathbf{0}, 0; 0) \text{ and } (\hat{\mathbf{u}}, \hat{p}; \gamma)\}. \quad \square \end{cases} \tag{34}$$

We will always suppose that the spaces U_h and P_h satisfy a condition even stronger than the *discrete inf-sup condition* (31). More precisely, we assume that the following *h-uniform discrete inf-sup condition* holds, for every γ:

$$\inf_{h>0} \left\{ \inf_{q_h \in P_h} \sup_{\mathbf{v}_h \in U_h} \frac{b_\gamma(\mathbf{v}_h, q_h)}{\|\mathbf{v}_h\|_U \|q_h\|_P} \right\} > 0. \tag{35}$$

This assumption is very reasonable, since for every γ it essentially corresponds to a classical inf–sup condition in the deformed configuration (see [16] for details). Therefore, a crucial role to determine the *discrete stability range* $S_h(\mathscr{P}_\gamma)$ will be played by the *h*-uniform discrete coercivity on the kernel condition. With this respect, we can now prove the following proposition.

Proposition 1. *Let $(\hat{\mathbf{u}}, \hat{p}) \in \widehat{U} \times \widehat{P}$ be a solution of Problem (8), for a given γ. Suppose that the corresponding bilinear form $a_\gamma(\cdot,\cdot)$ is indefinite on K_γ, i.e. (cf. (25))*

$$\alpha_\gamma := \inf_{\mathbf{v} \in K_\gamma} \frac{a_\gamma(\mathbf{v}, \mathbf{v})}{\|\mathbf{v}\|_U^2} < 0. \tag{36}$$

Then for the discrete counterpart (30) it holds

$$\inf_{h>0} \left\{ \inf_{\mathbf{v}_h \in K_{\gamma,h}} \frac{a_\gamma(\mathbf{v}_h, \mathbf{v}_h)}{\|\mathbf{v}_h\|_U^2} \right\} < 0, \tag{37}$$

where the discrete kernel $K_{\gamma,h}$ is defined by (33).

Proof. By (36) there exists $\tilde{\mathbf{v}} \in K_\gamma$ such that

$$\frac{a_\gamma(\tilde{\mathbf{v}}, \tilde{\mathbf{v}})}{\|\tilde{\mathbf{v}}\|_U^2} < 0. \tag{38}$$

The *h*-uniform discrete inf–sup condition (35) implies (see [8]):

$$\inf_{\mathbf{v}_h \in K_{\gamma,h}} \|\mathbf{v} - \mathbf{v}_h\|_U \leqslant C_\gamma \inf_{\mathbf{v}_h \in U_h} \|\mathbf{v} - \mathbf{v}_h\|_U \quad \forall \mathbf{v} \in K_\gamma. \tag{39}$$

Therefore, from (39) to (29) there exists $\tilde{\mathbf{v}}_h \in K_{\gamma,h}$ such that

$$\tilde{\mathbf{v}}_h \to \tilde{\mathbf{v}} \quad \text{in } U \quad \text{as } h \to 0. \tag{40}$$

Hence it holds, as $h \to 0$:

$$a_\gamma(\tilde{\mathbf{v}}_h, \tilde{\mathbf{v}}_h) \to a_\gamma(\tilde{\mathbf{v}}, \tilde{\mathbf{v}}) \quad \text{and} \quad \|\tilde{\mathbf{v}}_h\|_U^2 \to \|\tilde{\mathbf{v}}\|_U^2. \tag{41}$$

Estimate (37) now follows from (38) to (41). $\square$

Remark 2. Proposition 1 reveals that, apart very particular cases addressed in Remark 3, the discrete stability range is contained in the stability range for the continuous problem. Therefore, when a mixed conforming approximation is used, the pathology which may be expected in general is the following. It may happen that a discretization procedure detects a stability range which is strictly contained in the stability range for the continuous problem (cf. Definitions 1 and 2), even asymptotically as $h \to 0$. This means that the discretized problem might get unstable "too early" (see Fig. 2). Instances of such cases are investigated and presented in Section 5. Finally, we also remark that Proposition 1 does not imply that the stability range approximation *always* fails: situations showing an accurate discrete stability range might occur.

Remark 3. We remark that in very particular situations the numerical scheme could detect a larger stability range. This might happen only if the function $\gamma \to \alpha_\gamma$ exhibits a zero plateau region at the boundary of the stability range $S(\mathscr{P}_\gamma)$, as depicted in Fig. 3. We note that a zero plateau region may mechanically correspond to a region where the body is placed in *indifferent equilibrium* positions.

3.2. Approximation by means of the stream function formulation

We next consider a Galerkin approximation of Problem (19). We thus select a family of finite dimensional subspaces $\Phi_{\gamma,h} \subset \Phi_\gamma$ ($h > 0$), with the basic approximation property:

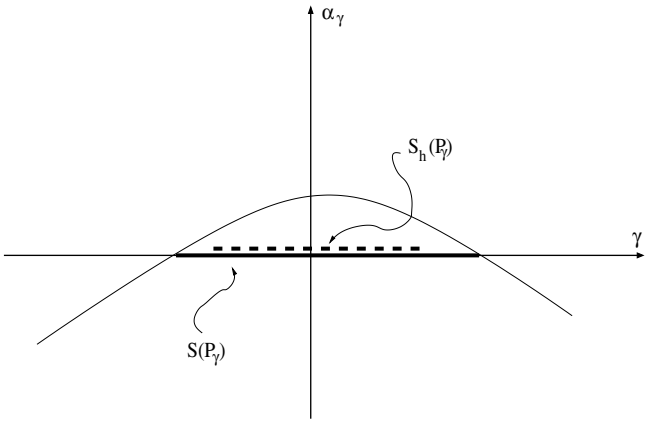

Fig. 2. A first possible pathology of the stability range for the mixed discretization with h "small" (dashed line). The stability range for the continuous problem is also displayed (solid line).

$$\bigcup_{h>0} \Phi_{\gamma,h} \text{ is dense in } \Phi_\gamma. \tag{42}$$

We then consider the following discrete problem:

$$\begin{cases} \text{Problem } (\mathscr{L}\mathscr{P}^*_{\gamma,h}) : \text{Find } \varphi_h \in \Phi_{\gamma,h} \text{ such that} \\ a^*_\gamma(\varphi_h, \psi_h) = \dfrac{\partial}{\partial\gamma}\mathscr{F}(\mathbf{curl}_{\widehat{\mathbf{F}}}\psi_h;\gamma)\delta\gamma \quad \forall \psi_h \in \Phi_{\gamma,h}. \end{cases} \tag{43}$$

Once $\varphi_h \in \Phi_{\gamma,h}$ has been found by solving (43), the displacement increment $\mathbf{u}_h$ can be obtained by computing

$$\mathbf{u}_h = \mathbf{curl}_{\widehat{\mathbf{F}}}\varphi_h. \tag{44}$$

Within this framework, the discrete counterparts of Definitions 1 and 2 becomes (cf. (27)).

Definition 5. Let $\gamma \in \mathscr{R}$, and let $(\hat{\mathbf{u}}, \hat{p}) \in U \times P$ be a solution to *Problem* $(\mathscr{P}_\gamma)$ (see (8)). For a given $h > 0$, we say that $(\hat{\mathbf{u}}, \hat{p}; \gamma)$ is a *discrete linearization stable point* for *Problem* $(\mathscr{P}_\gamma)$ if the corresponding discrete linearization (43) satisfies:

- *the discrete coercivity condition*, i.e. it holds

$$\inf_{\psi_h \in \Phi_{\gamma,h}} \frac{a^*_\gamma(\psi_h, \psi_h)}{\|\psi_h\|^2_{\Phi_\gamma}} > 0. \tag{45}$$

Definition 6. For a given $h > 0$, we define the *discrete stability range* of *Problem* $(\mathscr{P}_\gamma)$ as the interval $S^*_h(\mathscr{P}_\gamma) = (\gamma^*_{m,h}, \gamma^*_{M,h}) \subseteq \mathscr{R}$, where

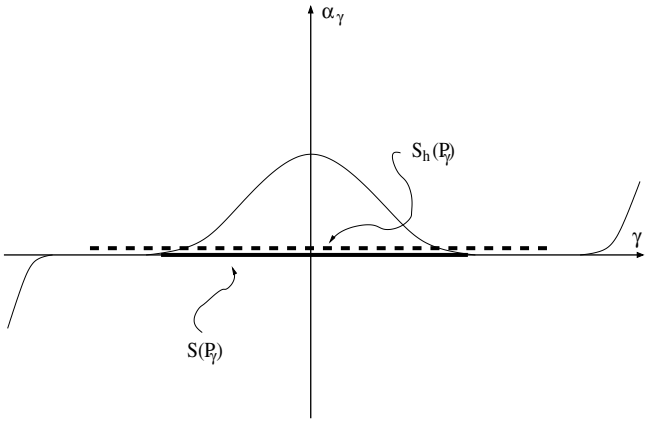

Fig. 3. A second possible pathology of the stability range for the mixed discretization with h "small" (dashed line). The stability range for the continuous problem is also displayed (solid line).

$$\begin{cases} \gamma^*_{m,h} = \inf\{\gamma \in \mathscr{R} : \exists \text{ a continuous path of discrete linearization} \\ \qquad \text{stable points joining } (\mathbf{0}, 0; 0) \text{ and } (\hat{\mathbf{u}}, \hat{p}; \gamma)\}, \\ \gamma^*_{M,h} = \sup\{\gamma \in \mathscr{R} : \exists \text{ a continuous path of discrete linearization} \\ \qquad \text{stable points joining}(\mathbf{0}, 0; 0) \text{ and } (\hat{\mathbf{u}}, \hat{p}; \gamma)\}. \quad \square \end{cases} \tag{46}$$

Proposition 4. *Let $(\hat{\mathbf{u}}, \hat{p}) \in \widehat{U} \times \widehat{P}$ be a solution of Problem (8), for a given γ. Consider the corresponding stream function formulation (19) and its discrete counterpart (43). Then it holds (cf. also (27))*

$$\alpha_\gamma := \inf_{\psi \in \Phi_\gamma} \frac{a^*_\gamma(\psi, \psi)}{\|\psi\|^2_{\Phi_\gamma}} = \inf_{h>0} \left\{ \inf_{\psi_h \in \Phi_{\gamma,h}} \frac{a^*_\gamma(\psi_h, \psi_h)}{\|\psi_h\|^2_{\Phi_\gamma}} \right\}. \tag{47}$$

Proof. We first set

$$\alpha_\gamma(h) := \inf_{\psi_h \in \Phi_{\gamma,h}} \frac{a^*_\gamma(\psi_h, \psi_h)}{\|\psi_h\|^2_{\Phi_\gamma}}. \tag{48}$$

Since $\Phi\gamma,h \subset \Phi\gamma$ for every $h > 0$, we have

$$\alpha_\gamma := \inf_{\psi \in \Phi_\gamma} \frac{a^*_\gamma(\psi, \psi)}{\|\psi\|^2_{\Phi_\gamma}} \leqslant \inf_{h>0}\{\alpha_\gamma(h)\}. \tag{49}$$

Suppose now that it holds

$$\alpha_\gamma < \inf_{h>0}\{\alpha_\gamma(h)\}. \tag{50}$$

Hence, there exists $\varepsilon > 0$ and a $\tilde{\psi} \in \Phi_\gamma$ (depending on ε) such that

$$\alpha_\gamma \leqslant \frac{a^*_\gamma(\tilde{\psi}, \tilde{\psi})}{\|\tilde{\psi}\|^2_{\Phi_\gamma}} < \alpha_\gamma + \varepsilon < \inf_{h>0}\{\alpha_\gamma(h)\}. \tag{51}$$

We now choose $\tilde{\psi}_h \in \Phi_{\gamma,h}$ as the best approximation of $\tilde{\psi}$ with respect to the $\Phi\gamma$-norm. On the one hand, from (51) we have

$$\alpha_\gamma \leqslant \frac{a^*_\gamma(\tilde{\psi}, \tilde{\psi})}{\|\tilde{\psi}\|^2_{\Phi_\gamma}} < \alpha_\gamma + \varepsilon < \inf_{h>0}\{\alpha_\gamma(h)\} \leqslant \frac{a^*_\gamma(\tilde{\psi}_h, \tilde{\psi}_h)}{\|\tilde{\psi}_h\|^2_{\Phi_\gamma}}. \tag{52}$$

On the other hand, since $\tilde{\psi}_h \to \tilde{\psi}$ in $\Phi\gamma$ as $h \to 0$ (cf. (42)), it holds

$$\lim_{h\to 0} \frac{a^*_\gamma(\tilde{\psi}_h, \tilde{\psi}_h)}{\|\tilde{\psi}_h\|^2_{\Phi_\gamma}} = \frac{a^*_\gamma(\tilde{\psi}, \tilde{\psi})}{\|\tilde{\psi}\|^2_{\Phi_\gamma}}. \tag{53}$$

A combination of (52) and (53) yields

$$\frac{a^*_\gamma(\tilde{\psi}, \tilde{\psi})}{\|\tilde{\psi}\|^2_{\Phi_\gamma}} < \alpha_\gamma + \varepsilon < \frac{a^*_\gamma(\tilde{\psi}, \tilde{\psi})}{\|\tilde{\psi}\|^2_{\Phi_\gamma}}, \tag{54}$$

which is clearly a contradiction. $\square$

Remark 5. Proposition 4 reveals that any reasonable conforming approximation of the linearized problem based on the "stream function" formulation is capable to correctly detect the stability range $S(\mathscr{P}_\gamma)$, at least asymptotically as $h \to 0$ (see Fig. 4). Indeed, Proposition 4 implies that $(\hat{\mathbf{u}}, \hat{p}; \gamma)$ is a linearization stable point if and only if it is a discrete linearization stable point for sufficiently small mesh sizes. As a consequence

$$S(\mathscr{P}_\gamma) = \bigcap_{h>0} S^*_h(\mathscr{P}_\gamma). \tag{55}$$

4. Two simple examples

In this section we present two *simple* problems which will be used in Section 5 to discuss on the performance of some numerical schemes in approximating the stability range $S(\mathscr{P}_\gamma)$. Using the

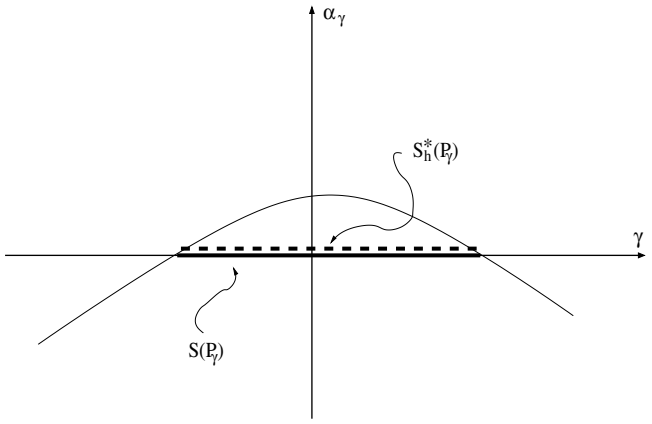

Fig. 4. Stability range for the stream-based discretization with h "small" (dashed line). The stability range for the continuous problem is also displayed (solid line).

usual Cartesian coordinates (X,Y), we consider a square material body whose reference configuration is $\Omega = (-1,1)\times(-1,1)$; we denote with $\Gamma = [-1,1]\times\{1\}$ the upper part of its boundary, while the remaining part of $\partial\Omega$ is denoted with Γ_D. The total energy is assumed to be as in (4), where the external loads are given by the vertical uniform body forces:

$$\mathscr{F}(\mathbf{v};\gamma) = \gamma \int_\Omega \mathbf{f}\cdot\mathbf{v}, \tag{56}$$

with $\mathbf{f} = (0,1)^T$. The two problems differ for the imposed boundary conditions. More precisely:

- **Problem 1.** We set clamped boundary conditions on Γ_D, traction-free boundary conditions on Γ (cf. Fig. 5(left)).
- **Problem 2.** We set vanishing normal displacements on Γ_D, traction-free boundary conditions on Γ (cf. Fig. 5(right)).

It is easy to see that both the problems admit a trivial solution *for every* $\gamma\in\mathbf{R}$, i.e. $(\hat{\mathbf{u}},\hat{p}) = (\mathbf{0},\gamma r)$, where $r = r(X,Y) = 1 - Y$.

For the problems under investigation, the corresponding linearized problems (cf. (10)) may both be written as

$$\begin{cases} \text{Problem } (\mathscr{L}\mathscr{P}_\gamma): \text{Find } (\mathbf{u},p)\in U\times P \text{ such that} \\ 2\mu\int_\Omega \boldsymbol{\varepsilon}(\mathbf{u}):\boldsymbol{\varepsilon}(\mathbf{v}) - \gamma\int_\Omega r(\nabla\mathbf{u})^T:\nabla\mathbf{v} + \int_\Omega p\,\mathrm{div}\,\mathbf{v} = \delta\gamma\int_\Omega \mathbf{f}\cdot\mathbf{v}, \\ \int_\Omega q\,\mathrm{div}\,\mathbf{u} = 0 \end{cases} \tag{57}$$

for every $(\mathbf{v},q)\in U\times P$. Accordingly with the two different problems, the spaces U and P are the following:

- **Problem 1**

$$U = \{\mathbf{v}\in H^1(\Omega)^2 : \mathbf{v}_{|\Gamma_D} = 0\}; P = L^2(\Omega). \tag{58}$$

- **Problem 2**

$$U = \{\mathbf{v}\in H^1(\Omega)^2 : (\mathbf{v}\cdot\mathbf{n})_{|\Gamma_D} = 0\}; \quad P = L^2(\Omega), \tag{59}$$

where $\mathbf{n}$ denotes the outward normal vector.

The "stream function" formulation reads as follows (see (19)):

$$\begin{cases} \text{Problem } \mathscr{L}\mathscr{P}^*_\gamma: \text{ Find } \varphi\in\Phi \text{ such that} \\ a^*_\gamma(\varphi,\psi) = \delta\gamma\int_\Omega \mathbf{f}\cdot\mathbf{curl}\,\psi \quad \forall\psi\in\Phi, \end{cases} \tag{60}$$

where

$$\begin{aligned} a^*_\gamma(\varphi,\psi) := {} & 2\mu\int_\Omega \boldsymbol{\varepsilon}(\mathbf{curl}\,\varphi):\boldsymbol{\varepsilon}(\mathbf{curl}\,\psi) \\ & - \gamma\int_\Omega r(\nabla(\mathbf{curl}\,\varphi))^T:\nabla(\mathbf{curl}\,\psi). \end{aligned} \tag{61}$$

Accordingly with the two different problems, the space Φ is the following:

- **Problem 1**

$$\Phi = \left\{\psi\in H^2(\Omega) : \psi = \frac{\partial\psi}{\partial\mathbf{n}} = 0 \quad \text{on } \Gamma_D\right\}. \tag{62}$$

- **Problem 2**

$$\Phi = \{\psi\in H^2(\Omega) : \psi = 0 \quad \text{on } \Gamma_D\}. \tag{63}$$

Remark 6. For Problem 1, it has been theoretically proved in [3] that the corresponding stability range $S(\mathscr{P}_\gamma)$ satisfies $(-\infty, 3\mu)\subseteq S(\mathscr{P}_\gamma)$.

5. Numerical results

In this section we report our numerical computations about the approximation of the stability range for the two problems detailed in Section 4. We first present the stream formulation results, since they provide an accurate approximation of the continuum stability range (cf. Proposition 4) and, therefore, they can be used as reliable reference solutions for the schemes based on the mixed formulation.

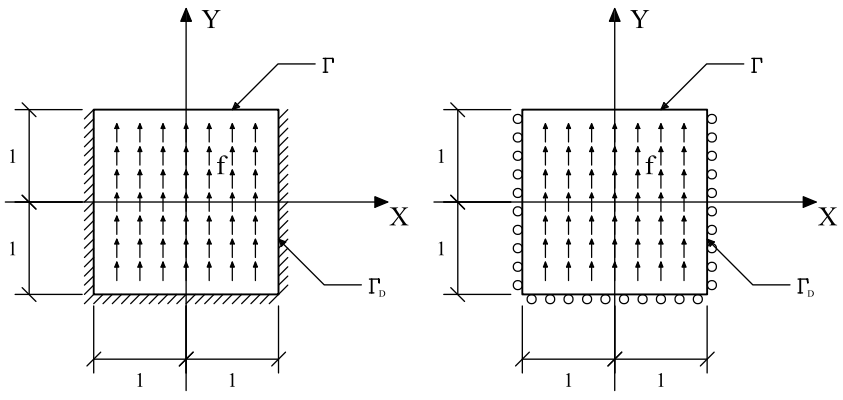

Fig. 5. Problem domain Ω.

5.1. NURBS for the stream function formulation

We assume that the physical domain Ω is a NURBS (see, e.g. [24,25]) region associated with a $n \times m$ net of control points $\mathbf{B}_{i,j}$, and we introduce the geometrical map $\mathbf{F} : [0,1] \times [0,1] \to \overline{\Omega}$ given by

$$\mathbf{F}(\xi,\eta) = \sum_{i=1}^{n} \sum_{j=1}^{m} R_{i,j}^{p,q}(\xi,\eta)\mathbf{B}_{i,j}, \tag{64}$$

where $R_{i,j}^{p,q}(\xi,\eta)$ are NURBS basis functions on the two-dimensional parametric space $[0,1] \times [0,1]$. The image of the elements in the parametric spaces are elements in the physical spaces. The physical mesh is therefore

$$\mathscr{T}_h = \{\mathbf{F}((\xi_i,\xi_{i+1}) \times (\eta_j,\eta_{j+1})) \text{ with } i = 1,\dots,n+p, \quad j = 1,\dots,m+q\}. \tag{65}$$

We denote by h the mesh-size, that is, the maximum diameter of the elements of $\mathscr{T}_h$.

Following the isoparametric approach, the space of NURBS functions on Ω is defined as the span of the *push-forward* of the basis functions $R_{i,j}^{p,q}(\xi,\eta)$

$$\mathscr{V}_h = \text{span}\{R_{i,j}^{p,q} \circ \mathbf{F}^{-1}\}_{i=1,\dots,n;\, j=1,\dots,m}. \tag{66}$$

This analysis framework is referred to as NURBS-based *isogeometric analysis*. The interested reader may find details and applications of isogeometric analysis for example in [4,6,10,11,13,14]; in particular, the approximation result (42) follows directly from the results of [6].

We introduce now the NURBS conforming discretization of the variational problem (60). Let $\mathscr{V}_h$ denote a NURBS space as introduced in (66), of regularity C^k, $k \geqslant 1$, and degree $p > k$. We have $\mathscr{V}_h \subset H^2(\Omega)$, and then we can introduce the following conforming discretizations of Φ

$$\Phi_h = \mathscr{V}_h \cap \Phi. \tag{67}$$

5.1.1. NURBS approximation: numerical results

We are now able to use the NURBS-based discretization introduced above in order to study the two model problems of Section 4, sketched in Fig. 5, and find sharp estimates for the continuum stability range $S(\mathscr{P}_\gamma)$ (cf. Proposition 4).

We highlight that to find critical loads we study the eigenvalues of the (loading parameter-dependent) stiffness matrix for the NURBS-based stream formulation described by (60)–(63) for the problems under consideration. Indeed, the quantity (cf. (45))

$$\inf_{\psi_h \in \Phi_{\gamma,h}} \frac{a_\gamma^*(\psi_h,\psi_h)}{\|\psi_h\|_{\Phi_\gamma}^2} \tag{68}$$

is a kind of Rayleigh quotient, whose sign is determined by the sign of the smallest eigenvalue of the matrix arising from the bilinear form $a_\gamma^*(\cdot,\cdot)$. The first loads for which we find a negative eigenvalue are the critical ones and, accordingly with Definition 6, they are indicated as $\gamma_{m,h}^*$ and $\gamma_{M,h}^*$, respectively.

Tables 1 and 2 report the results we found for the two problems. For different approximation degrees (and, precisely, for $p = q = 2,3,\dots,6$, being p and q the degrees in the two parametric directions) we used meshes of 4×4 to 32×32 elements. Due to the structure of the formulation (see [4]), this gives rise to $(n+p) \times (m+q)$ degrees-of-freedom (d.o.f.'s) for a mesh of $n \times m$ elements, so the total number of d.o.f.'s actually employed depends also on the approximation degrees (and is explicitly reported in the tables between brackets).

We moreover remark that, here and in the following, we express the numerical results in terms of the nondimensional quantity $\tilde{\gamma}_{m,h}^*$ (resp. $\tilde{\gamma}_{M,h}^*$) defined as $\tilde{\gamma}_{m,h}^* = \gamma_{m,h}^* L/\mu$ (resp. $\tilde{\gamma}_{M,h}^* = \gamma_{M,h}^* L/\mu$). Here, L is some problem characteristic length, set equal to 1 for simplicity, consistently also with the geometry of the model problems.

Table 1
Problem 1: critical load value $\tilde{\gamma}_{M,h}^*$ computed using the NURBS-based stream function formulation. The total number of employed d.o.f.'s is reported between brackets

Elements	$p = q$				
	2	3	4	5	6
4×4	7.96 (6×6)	6.88 (7×7)	6.71 (8×8)	6.65 (9×9)	6.63 (10×10)
8×8	7.08 (10×10)	6.67 (11×11)	6.63 (12×12)	6.61 (13×13)	6.61 (14×14)
16×16	6.75 (18×18)	6.62 (19×19)	6.61 (20×20)	6.61 (21×21)	6.61 (22×22)
32×32	6.65 (34×34)	6.61 (35×35)	6.60 (36×36)	6.60 (37×37)	6.60 (38×38)

Table 2
Problem 2: critical load value $\tilde{\gamma}_{M,h}^*$ computed using the NURBS-based stream function formulation

Elements	$p = q$				
	2	3	4	5	6
4×4	3.41 (6×6)	3.24 (7×7)	3.23 (8×8)	3.23 (9×9)	3.23 (10×10)
8×8	3.28 (10×10)	3.23 (11×11)	3.23 (12×12)	3.23 (13×13)	3.23 (14×14)
16×16	3.24 (18×18)	3.23 (19×19)	3.23 (20×20)	3.23 (21×21)	3.23 (22×22)
32×32	3.24 (34×34)	3.23 (35×35)	3.23 (36×36)	3.23 (37×37)	3.23 (38×38)

The total number of employed d.o.f.'s is reported between brackets.

In Tables 1 and 2, it is possible to observe excellent convergence paths both in h (i.e., mesh-refining) and in p (i.e., order-elevating). Therefore, recalling Remark 5, we can consider reliable the finest results obtained (i.e., for the case of degree $p = q = 6$ over a 32×32 mesh, corresponding to 38×38 d.o.f.'s), which are

- $\tilde{\gamma}_{M,h}^* = 6.60$ for Problem 1;
- $\tilde{\gamma}_{M,h}^* = 3.23$ for Problem 2.

In the following we indicate such results as "exact" (between quotes), referring to the fact that the stream function critical value converges to the one for the continuum problem, i.e. the exact one, as proved in Section 3.2.

We finally remark that we did not find any negative critical value (i.e., $\tilde{\gamma}_{m,h}^* = -\infty$), so, in the tables, we report only positive critical load values, $\tilde{\gamma}_{M,h}^*$. For Problem 1, this is in accordance with the theoretical result detailed in [3] (cf. also Remark 6).

5.2. Mixed finite elements

We consider here the discretized counterpart of problem (57), using some mixed finite element formulations which are known to optimally perform in the linear elastic framework. In the following, we briefly present the numerical schemes under consideration and we then show the numerical results obtained using such elements.

5.2.1. The MINI element

The first considered scheme is the MINI element (cf. [1]). Let $\mathscr{T}_h$ be a triangular mesh of Ω, h being the meshsize. For the discretization of the displacement field, we take

$$U_h = \{\mathbf{v}_h \in U : \mathbf{v}_{h|T} \in \mathscr{P}_1(T)^2 + \mathscr{B}(T)^2 \quad \forall T \in \mathscr{T}_h\}, \tag{69}$$

where $\mathscr{P}_1(T)$ is the space of linear functions on T, and $\mathscr{B}(T)$ is the linear space generated by b_T, the standard cubic bubble function on T. For the pressure discretization, we take

$$P_h = \{q_h \in H^1(\Omega) \cap P : q_{h|T} \in \mathscr{P}_1(T) \quad \forall T \in \mathscr{T}_h\}. \tag{70}$$

5.2.2. The $\mathscr{Q}_2/\mathscr{P}_1$ element

We now consider the $\mathscr{Q}_2/\mathscr{P}_1$ element (see [8]). Let $\mathscr{T}_h$ be a quadrilateral mesh of Ω, h being the meshsize. For the discretization of the displacement field, we take

$$U_h = \{\mathbf{v}_h \in U : \mathbf{v}_{h|K} \in \mathscr{Q}_2(K)^2 \quad \forall K \in \mathscr{T}_h\}, \tag{71}$$

where $\mathscr{Q}_2(K)$ is the standard space of biquadratic functions. For the pressure discretization, we take

$$P_h = \{q_h \in P : q_{h|K} \in \mathscr{P}_1(K) \quad \forall K \in \mathscr{T}_h\}. \tag{72}$$

5.2.3. The QME element

We now focus on the QME quadrilateral method proposed by Pantuso and Bathe in [22,23], based on the *Enhanced Strain Technique* [26]. This scheme optimally performs in small deformation regimes, as theoretically proved by [17]. Given $\mathscr{T}_h$, a quadrilateral mesh of Ω with meshsize h, the Pantuso–Bathe element is described by the following choice of spaces. For the discretization of the displacement field, we take

$$U_h = \{\mathbf{v}_h \in U : \mathbf{v}_{h|K} \in \mathscr{Q}_1(K)^2 \quad \forall K \in \mathscr{T}_h\}, \tag{73}$$

where $\mathscr{Q}_1(K)$ is the standard space of bilinear functions. For the pressure discretization, we take

$$P_h = \{q_h \in H^1(\Omega) \cap P : q_{h|K} \in \mathscr{Q}_1(K) \quad \forall K \in \mathscr{T}_h\}. \tag{74}$$

Furthermore, the *Enhanced Strain Technique* requires the introduction of an additional suitable *strain tensor* space, which in the present case is described by (see [23])

$$S_h = \{\mathbf{E}_h \in (L^2(\Omega))^4 : \mathbf{E}_{h|K} \in E_6(K) \quad \forall K \in \mathscr{T}_h\}. \tag{75}$$

Above, $E_6(K)$ is the space of tensor-valued functions defined on K, spanned by the following shape functions

$$\begin{bmatrix} \alpha_1\xi + \alpha_2\xi\eta; & \alpha_3\xi \\ \alpha_4\eta; & \alpha_5\eta + \alpha_6\xi\eta \end{bmatrix} \quad \text{with } \alpha_i \in \mathbf{R}, \tag{76}$$

where (ξ,η) denotes the standard local coordinates on K.

5.2.4. The $\mathscr{P}_1$-iso-$\mathscr{P}_2/\mathscr{P}_0$ element

The last considered scheme is the $\mathscr{P}_1$-*iso*-$\mathscr{P}_2/\mathscr{P}_0$ element (see [2]). Let $\mathscr{T}_h$ be a triangular mesh of Ω, h being the meshsize. Let $\mathscr{T}_{h/2}$ be a refined mesh, obtained by splitting each triangle of $\mathscr{T}_h$ using the edge midpoints. For the discretization of the displacement field, we take

$$U_h = \{\mathbf{v}_h \in U : \mathbf{v}_{h|T} \in \mathscr{P}_1(T)^2 \quad \forall T \in \mathscr{T}_{h/2}\}. \tag{77}$$

For the pressure discretization, we take

$$P_h = \{q_h \in P : q_{h|T} \in \mathscr{P}_0(T) \quad \forall T \in \mathscr{T}_h\}, \tag{78}$$

where $\mathscr{P}_0(T)$ is the standard space of constant functions.

5.2.5. Mixed finite elements: numerical results

We now study the stability range of the discretized model problems by means of the mixed finite element formulations briefly described above.

To find critical loads we again study the eigenvalues of the (loading parameter-dependent) stiffness matrices derived by expressions (57)–(59) for the problems under consideration. Accordingly with Definition 4, we indicate as the critical loads $\gamma_{m,h}$ and $\gamma_{M,h}$ the first load values for which we find an eigenvalue which changes its sign. Indeed, such a change of sign reveals the presence of a zero eigenvalue in system (30) for some value of γ in the interval determined by the last incremental step. A subsequent bisection-type procedure is used to increase the accuracy of the critical load detections. The corresponding nondimensional quantities are denotes with $\tilde{\gamma}^*_{m,h}$ and $\tilde{\gamma}^*_{M,h}$, respectively (cf. Section 5.1.1).

Table 3
Problem 1: critical load values computed using some mixed finite element formulations

Nodes	MINI		QME		$\mathscr{P}_1$-*iso*-$\mathscr{P}_2/\mathscr{P}_0$		$\mathscr{Q}_2/\mathscr{P}_1$	
	$\tilde{\gamma}_{m,h}$	$\tilde{\gamma}_{M,h}$	$\tilde{\gamma}_{m,h}$	$\tilde{\gamma}_{M,h}$	$\tilde{\gamma}_{m,h}$	$\tilde{\gamma}_{M,h}$	$\tilde{\gamma}_{m,h}$	$\tilde{\gamma}_{M,h}$
5×5	$-\infty$	1.29	−8.9	1.06	$-\infty$	1.54	$-\infty$	2.71
9×9	$-\infty$	1.23	−14.7	1.03	−225	1.21	−106	1.61
17×17	$-\infty$	1.17	−28.1	1.02	−240	1.10	−179	1.31
33×33	$-\infty$	1.11	−55.7	1.01	−428	1.06	−346	1.18
Stream [38×38 d.o.f.'s, $p = q = 6$]:					$\tilde{\gamma}^*_{m,h} = -\infty$		$\tilde{\gamma}^*_{M,h} = 6.60$	

On the last row, the "exact" critical value from the stream function formulation is reported.

Table 4
Problem 2: critical load values computed using some mixed finite element formulations

Nodes	MINI		QME		$\mathscr{P}_1$-*iso*-$\mathscr{P}_2/\mathscr{P}_0$		$\mathscr{Q}_2/\mathscr{P}_1$	
	$\tilde{\gamma}_{m,h}$	$\tilde{\gamma}_{M,h}$	$\tilde{\gamma}_{m,h}$	$\tilde{\gamma}_{M,h}$	$\tilde{\gamma}_{m,h}$	$\tilde{\gamma}_{M,h}$	$\tilde{\gamma}_{m,h}$	$\tilde{\gamma}_{M,h}$
5×5	$-\infty$	1.29	−8.8	1.05	−48.3	1.28	−42.1	1.40
9×9	$-\infty$	1.22	−14.8	1.02	−104	1.15	−85.6	1.22
17×17	$-\infty$	1.15	−28.2	1.02	−196	1.08	−172	1.14
33×33	$-\infty$	1.10	−55.8	1.01	−381	1.05	−342	1.10
Stream [38×38 d.o.f.'s, $p = q = 6$]:					$\tilde{\gamma}^*_{m,h} = -\infty$		$\tilde{\gamma}^*_{M,h} = 3.23$	

On the last row, the "exact" critical value from the stream function formulation is reported.

Table 5
Comparison among the "exact" positive critical load values and those obtained with the considered mixed finite element formulations over the finest mesh used (33×33 nodes)

Problem	"exact"	MINI		QME		$\mathscr{P}_1$-iso-$\mathscr{P}_2/\mathscr{P}_0$		$\mathscr{Q}_2/\mathscr{P}_1$	
	$\tilde{\gamma}^*_{M,h}$	$\tilde{\gamma}_{M,h}$	$\frac{\tilde{\gamma}_{M,h}}{\tilde{\gamma}^*_{M,h}}$	$\tilde{\gamma}_{M,h}$	$\frac{\tilde{\gamma}_{M,h}}{\tilde{\gamma}^*_{M,h}}$	$\tilde{\gamma}_{M,h}$	$\frac{\tilde{\gamma}_{M,h}}{\tilde{\gamma}^*_{M,h}}$	$\tilde{\gamma}_{M,h}$	$\frac{\tilde{\gamma}_{M,h}}{\tilde{\gamma}^*_{M,h}}$
1	6.60	1.11	16.8%	1.01	15.3%	1.06	16.1%	1.18	17.9%
2	3.23	1.10	34.1%	1.01	31.3%	1.05	32.5%	1.10	34.1%

In the following tables, we report the results we found for the two problems (cf. respectively, Tables 3 and 4), compared with the "exact" results obtained using the stream function formulation.

For what concerns the negative stability limit, we may observe that, despite only the MINI element seems to be stable even for very large compressive loads, all the elements are able to represent rather well the stability range at least asymptotically. Instead, when focusing on the positive stability limit, it is immediately clear that all the considered elements fail in reproducing the correct limit. In fact, as highlighted in Table 5, they show critical load values which are between the 15% and the 18% of the "exact" one for Problem 1 and between the 31% and the 34% for Problem 2.

Therefore, it is possible to conclude that, in both the studied model situations, all the investigated mixed finite element schemes fail in properly reproducing the stability range of the continuum problem.

6. Conclusions

Within the framework of finite elasticity for incompressible materials, in this paper we focus on the problem of the stability range approximation for the continuum problem linearization.

In particular, we show how to construct a reliable estimate for the continuum stability limit, which is a fundamental ingredient in order to assess the performance of a numerical scheme in reproducing the stability properties of the continuum problem. Such an estimate is obtained using an isogeometric stream function formulation on the linearized problem around the exact solution. This allows to exactly enforce the linearized incompressibility constraint, using the high regularity of NURBS shape functions.

We then consider a couple of model problems in order to study the performance of a number of mixed finite element schemes known to optimally behave in the small strain regime. Our numerical tests show that, on the model problems, all the considered finite elements completely fail in reproducing the continuum stability range.

Therefore, we may conclude that, when dealing with highly constrained finite elasticity problems, the natural extensions of finite element schemes well performing in small strains are not guaranteed to correctly reproduce the stability range of the continuum problem. In fact, it seems to be a crucial issue the capability of the method to satisfy the internal constraints exactly, in particular when dealing with the incompressibility constraint. However, we remark that different approaches, such as the ones presented in [27–29] and in [15,20], could lead to reliable approximations and deserve investigations.

Acknowledgements

The authors would like to thank Professor T.J.R. Hughes, University of Texas at Austin, and Professor R.L. Taylor, University of California at Berkeley, for very valuable discussions on the subject of this paper.

A. Reali was partially supported by Regione Lombardia through the INGENIO research program No. A0000800. F. Auricchio and A. Reali were partially supported by the Ministero dell'Università e della Ricerca (MiUR) through the PRIN 2006 research program No. 2006083795. These supports are gratefully acknowledged.

References

[1] D.N. Arnold, F. Brezzi, M. Fortin, A stable finite element for the Stokes equation, Calcolo 21 (1984) 337–344.
[2] F. Auricchio, F. Brezzi, C. Lovadina, Mixed finite element methods, in: E. Stein, R. De Borst, T.J.R. Hughes (Eds.), Encyclopedia of Computational Mechanics, vol. 1, John Wiley and Sons, 2004 (Chapter 9).
[3] F. Auricchio, L. Beirão da Veiga, C. Lovadina, A. Reali, A stability study of some mixed finite elements for large deformation elasticity problems, Comput. Methods Appl. Mech. Engrg. 194 (2005) 1075–1092.
[4] F. Auricchio, L. Beirão da Veiga, A. Buffa, C. Lovadina, A. Reali, G. Sangalli, A fully "locking-free" isogeometric approach for plane linear elasticity problems: a stream function formulation, Comput. Methods Appl. Mech. Engrg. 197 (2007) 160–172.
[5] F. Auricchio, L. Beirão da Veiga, C. Lovadina, A. Reali, Stability of some finite element methods for finite elasticity problems, in: C. Carstensen, P. Wriggers, (Eds.), Mixed Finite Element Technologies, CISM Courses and Lectures, Springer, in press.
[6] Y. Bazilevs, L. Beirão de Veiga, J.A. Cottrell, T.J.R. Hughes, G. Sangalli, Isogeometric analysis: approximation, stability and error estimates for *h*-refined meshes, Math. Models Methods Appl. Sci. 16 (2006) 1–60.
[7] J. Bonet, R.D. Wood, Nonlinear Continuum Mechanics for Finite Element Analysis, Cambridge University Press, 1997.
[8] F. Brezzi, M. Fortin, Mixed and Hybrid Finite Element Methods, Springer-Verlag, New York, 1991.
[9] P.G. Ciarlet, Mathematical Elasticity, Three Dimensional Elasticity, vol. 1, North-Holland, Amsterdam, 1998.
[10] J.A. Cottrell, A. Reali, Y. Bazilevs, T.J.R. Hughes, Isogeometric analysis of structural vibrations, Comput. Methods Appl. Mech. Engrg. 195 (2006) 5257–5296.
[11] J.A. Cottrell, T.J.R. Hughes, A. Reali, Studies of refinement and continuity in isogeometric structural analysis, Comput. Methods Appl. Mech. Engrg. 196 (2007) 4160–4183.
[12] M.E. Gurtin, An Introduction to Continuum Mechanics, Academic Press, New York, 1981.
[13] T.J.R. Hughes, J.A. Cottrell, Y. Bazilevs, Isogeometric analysis: CAD, finite elements, NURBS, exact geometry, and mesh refinement, Comput. Methods Appl. Mech. Engrg. 194 (2005) 4135–4195.
[14] T.J.R. Hughes, A. Reali, G. Sangalli, Duality and unified analysis of discrete approximations in structural dynamics and wave propagation: comparison of *p*-method finite elements with *k*-method NURBS, Comput. Methods Appl. Mech. Engrg. 197 (2008) 4104–4124.
[15] O. Klaas, A.M. Maniatty, M.S. Shephard, A stabilized mixed Petrov–Galerkin finite element method for finite elasticity. formulation for linear displacement and pressure interpolation, Comput. Methods Appl. Mech. Engrg. 180 (1999) 65–79.
[16] P. Le Tallec, Numerical Methods for nonlinear three-dimensional elasticity, in: Handbook of Numerical Analysis, vol. 3, 1994, pp. 465–622.
[17] C. Lovadina, Analysis of strain–pressure finite element methods for the Stokes problem, Numer. Methods PDE's 13 (1997) 717–730.
[18] C. Lovadina, F. Auricchio, On the enhanced strain technique for elasticity problems, Comput. Struct. 81 (2003) 777–787.
[19] L.E. Malvern, Introduction to the Mechanics of a Continuous Medium, Prentice-Hall, Englewood Cliffs, NJ, 1969.
[20] A.M. Maniatty, Y. Liu, O. Klaas, M.S. Shephard, Higher order stabilized finite element method for hyperelastic finite deformation, Comput Methods Appl. Mech. Engrg. 191 (2002) 1491–1503.
[21] J.E. Marsden, T.J.R. Hughes, Mathematical Foundations of Elasticity, Dover Publications, NY, 1993.
[22] D. Pantuso, K.J. Bathe, A four-node quadrilateral mixed-interpolated element for solids and fluids, Math. Models Methods Appl. Sci. 5 (1995) 1113–1128.
[23] D. Pantuso, K.J. Bathe, On the stability of mixed finite elements in large strain analysis of incompressible solids, Finite Elements Anal. Des. 28 (1997) 83–104.
[24] L. Piegl, W. Tiller, The NURBS Book, second ed., Springer-Verlag, 1997.
[25] D.F. Rogers, An Introduction to NURBS with Historical Perspective, Academic Press, 2001.

[26] J.C. Simo, M.S. Rifai, A class of mixed assumed strain methods and the method of incompatible modes, Int. J. Numer. Methods Engng. 29 (1990) 1595–1638.
[27] A. Ten Eyck, A. Lew, Discontinuous Galerkin methods for nonlinear elasticity, Int. J. Numer. Methods Engng. 67 (2006) 1204–1243.
[28] A. Ten Eyck, F. Celiker, A. Lew, Adaptive stabilization of discontinuous Galerkin methods for nonlinear elasticity: motivation, formulation and numerical examples, Comput. Methods Appl. Mech. Engrg. 197 (2008) 3605–3622.
[29] A. Ten Eyck, F. Celiker, A. Lew, Adaptive stabilization of discontinuous Galerkin methods for nonlinear elasticity: analytical estimates, Comput. Methods Appl. Mech. Engrg. 197 (2008) 2989–3000.
[30] P. Wriggers, S. Reese, A note on enhanced strain methods for large deformations, Comput. Methods Appl. Mech. Engrg. 135 (1996) 201–209.